The Journal of Engineering

The 14th International Conference on Developments in Power System Protection (DPSP 2018)

IET Journals
The Institution of Engineering and Technology

Protection assessment in electrical distribution grids based on state estimation

eISSN 2051-3305
Received on 2nd May 2018
Accepted on 23rd May 2018
doi: 10.1049/joe.2018.0159
www.ietdl.org

Thomas Offergeld[1] ✉, Moritz Cramer[1], Felix Glinka[1], Armin Schnettler[1]

[1]*Institute for High Voltage Technology, RWTH Aachen University, Aachen, Germany*

✉ *E-mail: offergeld@ifht.rwth-aachen.de*

Abstract: The increasing number of inverter interfaced distributed generation units in electrical distribution grids can influence the functionality of protective devices in case of grid faults. The result can be an inadmissible delay in tripping time or failure to trip altogether. This study describes a novel approach to identify and amend potentially unreliable protection configurations. Reliance on conservative worst-case approximations of the grid state is avoided by using distribution system state estimation instead. Thereby, protection configurations can be more accurately matched to the specific grids' requirements. The overall computational effort is reduced using methods of regression analysis while maintaining original accuracy.

1 Introduction

Installation of distributed generation (DGs) units in distribution grids in the wake of the German 'Energiewende' leads to challenges in grid operation and planning for undisturbed operation and in case of faults in the grid.

While these challenges in the undisturbed operation are characterised by voltage band violations and transformer overloading in times of high feed-in, DG can impinge upon PDs' ability to clear a fault in their protective zone within permissible time. Eventually, this can cause asset damage or endanger members of the public.

Traditionally, German low voltage (LV) feeders are protected by fuses installed at the LV busbar of the distribution substation and occasionally additionally at select intermediary distribution cabinets [1].

The fuse characteristic is chosen appropriately to protect the assets that are installed downstream of the fuse. If the fault current fails to exceed the fuse's tripping threshold, no trip will occur and the fault will be allowed to persist, potentially creating a hazardous environment.

2 Fault properties and influencing factors

Disregarding inverter interfaced DG (IIDG), the minimal fault current is predominantly a function of fault location, fault type (i.e. single phase to ground or phase to phase) and fault impedance. By factorial combination of these properties, the fault cases that are investigated in this submission are defined (cf. Fig. 1).

DG units situated within the protective zone of a protective device can reduce the fault current experienced by the fuse ('*Blinding*') when a fault occurs within this very protective zone [2]. This reduction is determined by the IIDG control scheme and its pre-fault operating point.

In order to assess the suitability of installed PDs, the above influencing factors are taken into account together with the IIDG's pre-fault operating point. Minimum fault currents $I_{F,\min}$ show a high sensitivity towards the fault impedance Z_F and the distance between the fault and the grid-building generators [2].

Due to the rarity and randomness of faults, realistic fault impedances are difficult to determine. Therefore, this submission considers a multitude of potential fault impedances as one axis of the cube of fault cases. Additionally, the fault location is varied across all nodes of the grid model. Single phase-to-ground and phase-to-phase faults are considered.

Power injection from IIDGs will increase the voltage drop across any non-zero-impedance fault nearby. This leads to a more level slope in the feeder's voltage profile from the location of the grid-building generators to the fault location, decreasing the fault current supplied by the grid-building generators. Grid guidelines aim to counteract this by compelling IIDG to disconnect from the grid during prolonged voltage dips [3]. However, some combinations of fault properties and pre-fault states still cause the IIDG to remain connected and prohibit overcurrent tripping.

The described behaviour in terms of the quasi-steady-state fault current is shown in Fig. 2 for an exemplary test grid with a single IIDG. Fault currents across the fuse are evaluated for several combinations of discrete fault impedances Z_F and IIDG pre-fault infeed power P_{IIDG}. Fault currents $I_F = 0$ A suggest a successful fault clearance by the feeder fuse. Fault currents $I_F > 0$ represent failure to clear the fault as the fuse is not tripped and the fault current is allowed to persist.

For a fixed fault location, the fuse at the LV busbar is exposed to decreasing fault currents with an increase in available pre-fault power feed-in from a single IIDG. This reduction in fault current can lead to failures to pick up the fault current at the PDs, severely delaying or prohibiting entirely the tripping of the PDs. As can be observed for this specific test grid, increasing IIDG feed-in leads to failing fault clearance for fault impedances of $Z_F \geq 250$ mΩ. This impedance threshold depends on grid structure, locations of DG, grid parameters and the PD characteristics.

Therefore, to accurately assess the likelihood of a protective device failure, pre-fault power injection needs to be determined. The method used to incorporate these pre-fault system states into a protective device assessment is described in the following.

3 Distribution system state estimation

State estimation is a method most commonly used in transmission grids to deduct the most probable grid state (defined by voltages and current flows) from a redundant set of measurements creating an overdetermined system. In distribution systems, however, measurements are much more sparsely distributed. The resulting system of equations is heavily underdetermined. Only through use of supplementary artificial information (e.g. pseudo-measurements) the grid state can be extracted [4].

The investigations presented use real-world LV grids equipped with few node voltage, line current and line apparent power measurements with a temporal resolution of 1 s. The measurements are stored in a database and retrieved from there. The grids assessed are rural LV grids with known topology and locations of major DG.

The method for state estimation is displayed in Fig. 3. Grid topology and electrical properties (line lengths and impedances) are provided by the distribution system operator.

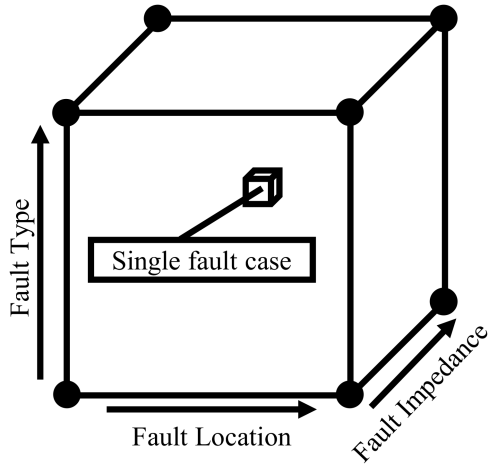

Fig. 1 *Concept of fault cases in factorial combinations*

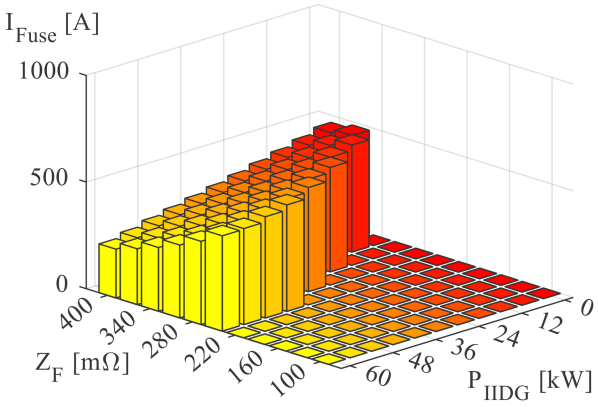

Fig. 2 *Fault current for an exemplary grid with IIDG after potential fuse trip*

Alongside real- and pseudo-measurements these properties are fed into the weighted least squares (WLS) state estimation. The state estimation uses a three-phase asymmetric branch-current based WLS estimator to determine the network state as a collection of complex voltages at the reference bus and complex line currents [5]. The estimation is an iterative minimisation of the weighted squared measurement error

$$\min J(x) = \min \sum w_i(z_i - h_i(x))^2 \qquad (1)$$

where w_i and $h_i(x)$ represent the measurement weight and the measurement function, respectively, for measurement z_i for step x [6]. This results in a state vector containing complex reference node voltage and branch current. From there, all node voltages, line power flows and power injections are calculated.

The system state is determined through state estimation every 15 min with measurement data being 15 min sliding average root mean square values, aggregated on the measurement database.

4 Quasi-steady-state short-circuit calculation

A main impact IIDG have on fault currents in LV grids is the aforementioned reduction of minimum fault current at the location of feeder protective devices. With the inverse time characteristic of fuses, a reduced fault current across the fuse leads to prolonged clearing times. Hence, *event-based* quasi-steady-state approximations for short-circuit calculations (SCCs) can decrease computational complexity while maintaining satisfactory accuracy [7]. The simulated time is divided into distinct time slices with *events* separating the slices from each other. The simulation flowchart is shown in Fig. 4.

The pre-fault state is determined through state estimation and constitutes the first time slice up to the first event (fault occurence). In the following slice, the fault is simulated by modification of the

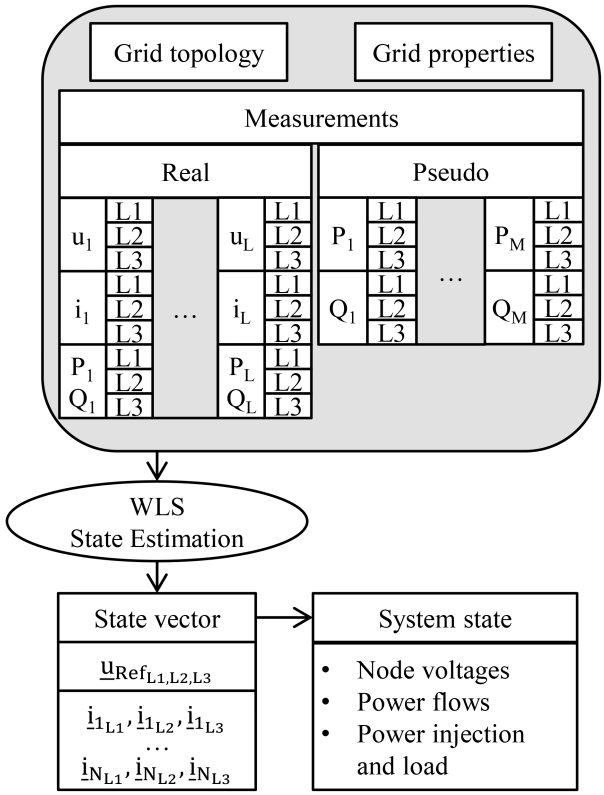

Fig. 3 *State estimation methodology*

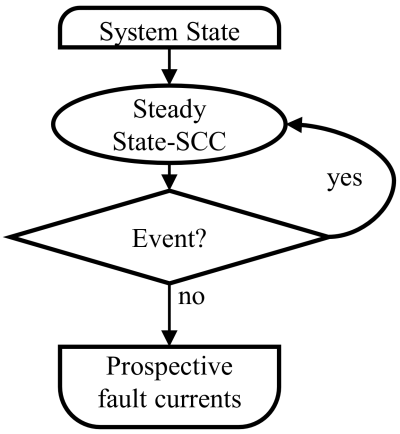

Fig. 4 *Event-based steady-state SCC*

nodal admittance matrix, and fault currents throughout the grid are calculated. IIDGs are modelled as current sources with a voltage dependency. That is, the injected reactive current is a function of voltage at the point of common coupling (PCC), inverter power rating and grid guidelines. The active current is a function of voltage at the PCC and remaining inverter power capacity after prioritisation of reactive current. Currents from different IIDGs and the higher voltage grid are superimposed until a stable operating point for voltage controlled current sources is found by iteration [7].

Under-voltage and over-voltage, and anti-islanding relays determine whether IIDGs stay connected during faults and are parametrised according to German grid regulations [3].

The fault current at fault location I_F, the fault current at the fuse protecting a feeder with IIDG, I_{PD}, and the excitation events are shown for a high impedance fault within the feeder in Table 1. The first slice containing the healthy system state extends to $t = 0$ s. The slice delimited by 0 and 0.2 s describes the first fault slice during which both the higher voltage grid and the IIDG feed a fault current into the fault. The fault current at the fuse I_{PD} does not exceed the excitation threshold of 500 A. Thus, the fuse does not undergo excitation. Only after the under-voltage relay (UR)

Table 1 Exemplary event sequence for successful clearance

t, s	Event	Currents, A I_F	I_{PD}
0	• fault occurs • excitation: IIDG UR	670	483
0.2	• trip: IIDG UR • excitation: feeder fuse	569	569
1600	• trip: feeder fuse	0	0

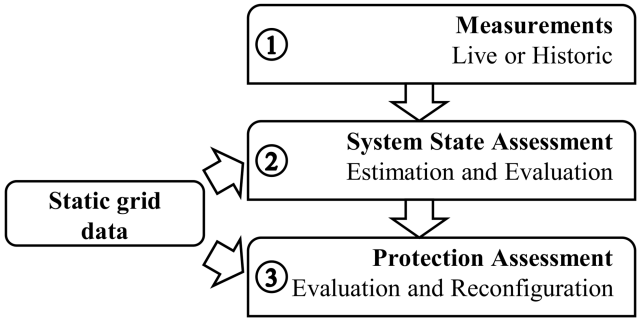

Fig. 5 *Basic methodology*

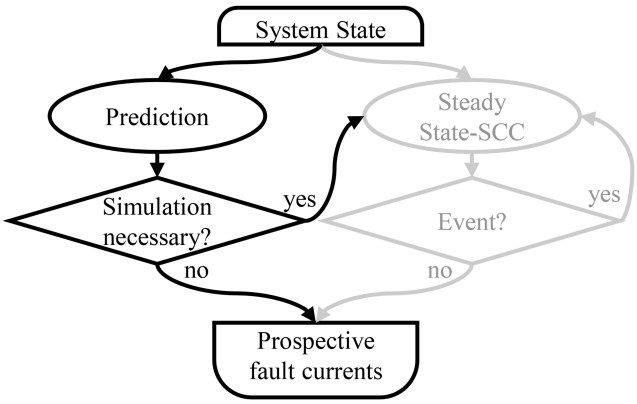

Fig. 8 *Modified short-circuit current determination*

disconnects the IIDG from the grid ($t = 0.2$ s), the fuse undergoes excitation. The fault is then cleared after 1600 s.

In some fault cases, the fault remains undetected by the UR as the voltage drop at the PCC is insufficient. Hence, the IIDG stay connected and the fuse threshold is never reached, resulting in blinding as seen in Fig. 2.

5 Protection assessment

The suitability of the installed protection scheme is assessed for different grid states and a multitude of different hypothetical fault cases (cf. Fig. 1).

The basic methodology is illustrated in Fig. 5. Grid states are taken chronologically from the measurement database described previously (1) and fed into the System State Assessment (2). The measurements are supplemented with pseudo-measurements and the most likely system state is estimated. Finally, the fault cases are simulated using the method described.

After simulation of all fault cases for this system state, the results are used to assess the protective devices' ability to clear a hypothetical fault in this very system state. For all fault cases that have not been cleared in the simulation (identified by non-zero fault current at the fault location), the responsible PDs are determined. For radial networks, where all DG units are equipped with anti-islanding protection and disconnect once their point of coupling becomes islanded, the responsible fuses are usually located upstream of the fault location at the secondary side busbar of the transformer. The responsibility of PDs to clear a fault is derived from their protective zones as shown in Fig. 6.

Assuming a connection to a higher voltage grid exists via node 0 a fault at nodes 2, 4 and 5 must be cleared by PD R1. Therefore,

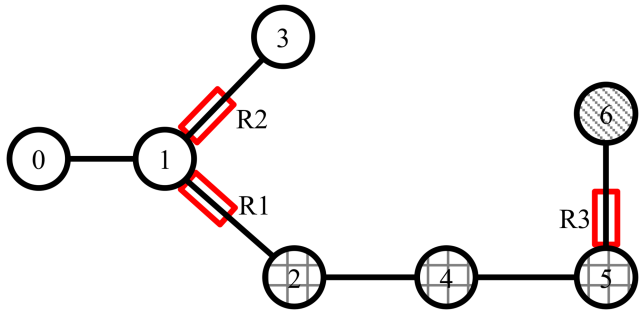

Fig. 6 *Concept of PD responsibility*

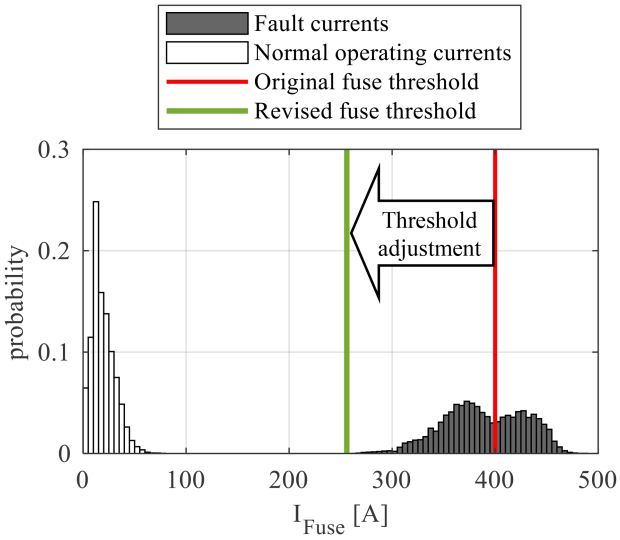

Fig. 7 *Exemplary fuse reconfiguration*

R1 is responsible for any uncleared faults at these nodes. For a fault at node 6, R3 or R1 must trip. However, to achieve maximum selectivity, R3 should trip before R1, leaving nodes 2, 4 and 5 connected to the grid.

After assessment of a predefined number of system states, reconfiguration recommendations for the protective devices that could be affected by blinding are derived. The number of system states spans multiple days to capture the volatility of generation from renewable sources. Reconfiguration attempts are repeated throughout the year to account for seasonal fluctuations.

6 Protection reconfiguration

To minimise the risk of a fuse failing to trip in case of a fault due to blinding as well as to avoid undue tripping in times of high loading, the reconfiguration recommendations are based on minimum prospective fault currents and maximum observed currents in normal operating states.

An exemplary reconfiguration is shown in Fig. 7. For the observed PD, the prospective fault currents occasionally fall short of the installed tripping threshold. Thus, in order to ensure tripping even when the fault current is reduced by blinding, the threshold has to be adjusted. To avoid undesired tripping due to high (but still admissible) loading currents, the normal operating currents are taken into account also.

While normal operating currents do not impose a high lower bound on the revised threshold in this specific example, peak loading currents might increase in the future with potential electrification of other energy sectors such as mobility and heating.

7 Computational efficiency considerations

Considering the high number of possible fault cases and system states, the computational complexity of developing the described reconfigurations is a measure of the method's feasibility for real-world applications. A number of LV grids are already equipped with intelligence for grid operational purposes [8]. However,

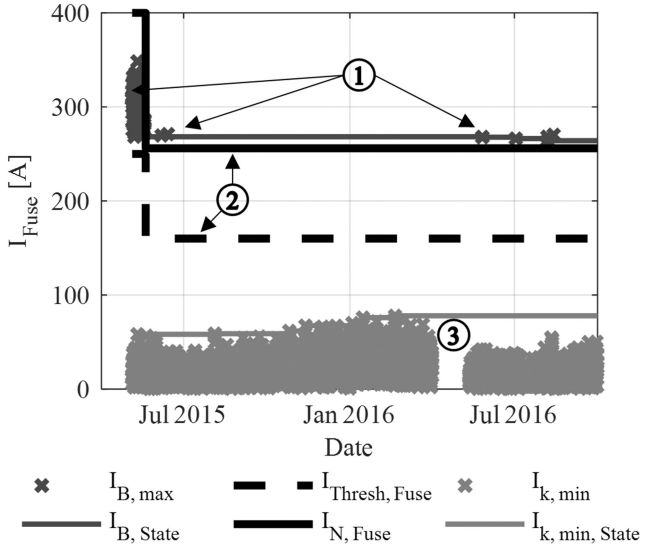

Fig. 9 *Assessment of overcurrent PD*

simulating all conceivable fault cases for every system state quickly becomes infeasible due to their high number. Instead, the proposed method implements an algorithm to reduce the number of cases to simulate for each system state by predicting the value of new information that could be gained by simulating these cases. A relation between the system state and the minimum fault current across each overcurrent PD is established by means of regression analysis after a predefined number of system states have been evaluated

$$I_{F,\text{Predicted}} = f\left(I_{\text{PD,pre-fault}}\right) \tag{2}$$

A linear regression model uses the pre-fault currents across each PD to predict the smallest fault current any fault case would cause across this PD. Hence, the previously described method for determination of prospective minimal short-circuit currents is replaced by a prediction as shown in Fig. 8, where only fault cases potentially yielding new minimum fault currents necessitate the time-consuming calculation of short-circuit currents.

To ensure accuracy, the prospective fault currents are classified into two distinct groups:

(a) $I_{\text{F,Predicted}} > m * I_{\text{Thresh}} + \min\left(I_{\text{F,min}}; I_{\text{Thresh}}\right)$
(b) $I_{\text{F,Predicted}} \leq m * I_{\text{Thresh}} + \min\left(I_{\text{F,min}}; I_{\text{Thresh}}\right)$

where $I_{\text{F,Predicted}}$ is an estimate of the minimal hypothetical fault current across this PD in the currently evaluated system state, I_{Thresh} is the PD's set-point threshold, m is a safety margin chosen to be 5% and $I_{\text{F,min}}$ is the lowest hypothetical fault current across this PD in all states up to the previous one.

Predictions satisfying condition (a) are skipped for calculation as no new information regarding minimum fault currents for a potential reconfiguration are expected to result from a calculation.

Predictions satisfying condition (b) however are not simply retained but instead, the fault cases are simulated in detail to maintain high accuracy of the results for a potential PD reconfiguration and predictions are replaced with exact results.

This regression model is updated periodically to increase its accuracy and to account for seasonal effects.

8 Exemplary results

The proposed method is applied to real-world LV grids containing photovoltaic IIDG and sufficient amount of historic measurement data to determine years' worth of grid states. The grids' overcurrent protective devices are LV fuses installed at the LV busbar and distribution cabinets. The fuse parameters in the simulation mirror the fuses currently installed in the grid. The under-voltage, over-

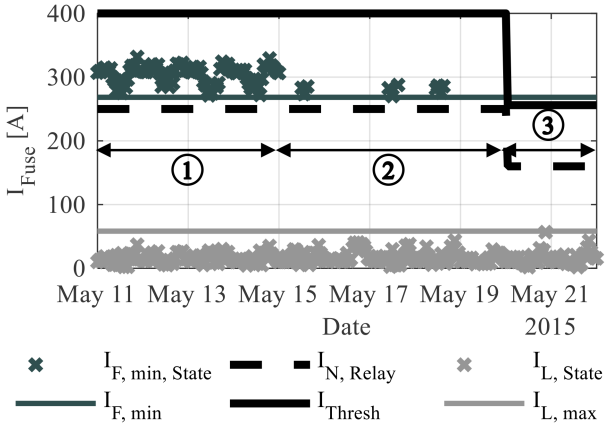

Fig. 10 *Initial assessment of overcurrent PD*

voltage and anti-island relays are configured in accordance with German grid guidelines.

Fig. 9 shows an assessment for a fuse installed at the busbar end of a long feeder with mixed generation and load with a short period of unavailable measurements which is skipped for assessments. The minimum fault currents this fuse is responsible to clear are shown at the top of the axes (1). The minimum fault current up to a certain time is shown as an enveloping line extending to about 260 A. Similarly, the loading current and the maximum loading current up to a time t are shown in light grey at the bottom of the axes (3). The fuse's nominal current (dashed black line) and its tripping threshold (solid black line) including a reconfiguration after 15 days are also shown (2). After the reconfiguration, minimum fault currents for the fault cases considered always exceed the revised tripping threshold, ensuring fault clearance.

A reduction of fault cases evaluated is evident from the reduction of newly found minimal fault currents thanks to the regression model. After reconfiguration, only very few fault cases are predicted to cause a fault current below the imposed criterion for calculation.

Fig. 10 shows the assessments within the first month of operation. The renewable volatility's effect on the fuse suitability can be seen as minimum potential fault currents vary during the day. This confirms that the behaviour displayed in Fig. 2 also occurs in real LV grids.

After 10 days (1), the regression model is established. Henceforth the number of cases evaluated is reduced to only system states where small fault currents are expected, resulting in larger gaps between determined minimum fault currents (2). After reconfiguration (3), the new fuse threshold is the new lower bound for the decision to calculate the fault cases for the system states. Since the predicted fault currents do not change significantly, almost no calculations for the cases pertaining this fuse are deemed necessary.

The reduction of computational effort for the entire grid is assessed by comparing the number of fault cases that need to be evaluated per system state on average for a margin of 5%.

Up until the first iteration of building the regression model, 100% of fault cases are evaluated by calculation. From there up until the first reconfiguration of fuses, 10.13% of fault cases are explicitly calculated. Beyond the only reconfiguration of fuses, 0.86% of fault cases necessitate calculation. The validity of results with this reduced computational effort is evaluated by comparing the enveloping minimum fault currents depicted in Figs. 9 and 10. The observed dependence between pre-fault currents and prospective fault currents for the fuse investigated before is shown in Fig. 11 showing strong correlation ($r = 99.66\%$).

The prediction error shown in Fig. 12 is small relative to the fuse threshold. Since the predictions are used only to decide whether fault cases are calculated, all fault cases causing an updated smallest fault current are simulated. Therefore, the effective error caused by the reduction of simulated fault cases is nil.

A reduction of the margin used for this decision to 1% leads to a further decrease in computational effort, however at the expense

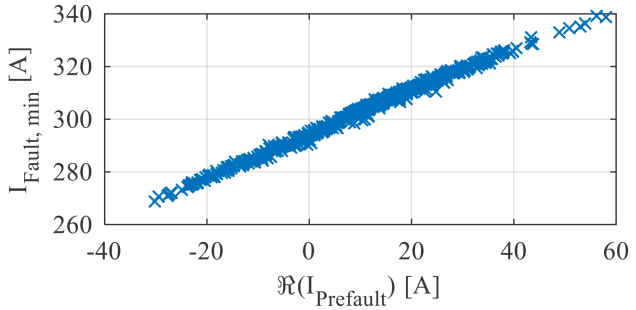

Fig. 11 *Correlation of pre-fault and hypothetical fault current*

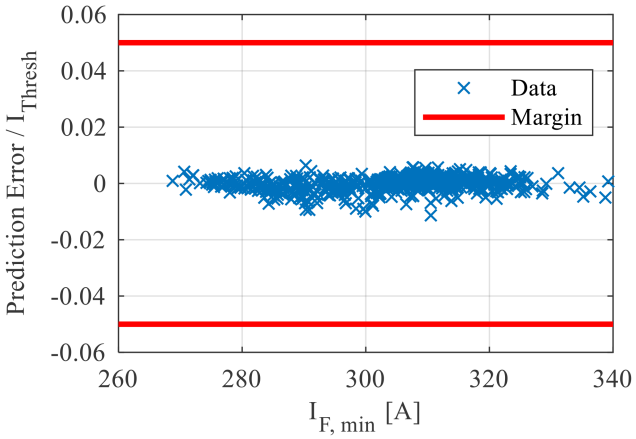

Fig. 12 *Relative prediction error and prospective minimum fault currents*

of accuracy. The absolute effective error regarding the minimum fault current increases from 0 to 3% of the relay's threshold current. In the grids assessed by this method, a margin of 5% has proven sufficient to detect potentially new minimum fault currents while reducing the computational complexity significantly.

9 Conclusion and outlook

The presented method successfully develops and simulatively implements reconfiguration proposals for overcurrent PDs. The configurations identified reduce the risk of faults remaining uncleared due to low fault currents fostered by high IIDG feed-in.

The issue of computational complexity is addressed and significant reduction is achieved through individual regression models establishing a relationship between pre-fault system states and hypothetical fault currents.

The proposed method can be used to automatically screen existing grids and their protection configuration for potential issues related to low fault currents and suggest adaptations in the protection configuration to address these issues.

A conjunction with probabilistic power flow calculations could be developed to enable using the method to plan protection configurations from scratch without relying on assumptions regarding the pre-fault system states or estimations requiring distributed measurements [9]. Especially if peak load currents increase due to the electrification of other energy sectors an individualised protection configuration becomes increasingly important as the gap between normal operating currents and fault currents closes.

10 References

[1] Neusel-Lange, N.: 'Dezentrale zustandsüberwachung für intelligente niederspannungsnetze', Dissertation, Bergische Universität Wuppertal, Wuppertal, 2013 (in German)

[2] Glinka, F., Bertram, R., Wippenbeck, T., *et al.*: 'Protection of today's and future low voltage grids with high DG penetration: laboratory and simulative analysis of blinding of protection with inverters'. 13th Int. Conf. on Development in Power System Protection, Edinburgh, 2016

[3] Verband der Elektrotechnik, Elektronik, Informationstechnik e.V. (VDE), Erzeugungsanlangen am Niederspannungsnetz - Technische Mindestanforderungen für Anschluss und Parallelbetrieb von Erzeugungsanlagen am Niederspannungsnetz, 2011 (in German)

[4] Cramer, M., Goergens, P., Potratz, F., *et al.*: 'Establishing transparency for distribution grid planning and operation using methods of state estimation'. CIRED Workshop, Helsinki, 2016

[5] Baran, M.E., Kelley, A.W.: 'A branch-current-based state estimation method for distribution systems', *IEEE Trans. Power Syst.*, 1995, **10**, (1), pp. 483–491

[6] Abur, A., Exposito, A.G.: '*Power system state estimation: theory and implementation*' (Marcel Dekker Inc, Hoboken, 2004)

[7] Wippenbeck, T., Jäkel, M., Schmidt, T., *et al.*: 'Development and cross-validation of short-circuit calculation methods for distribution grids with high penetration of inverter-interfaced distributed generation'. 23rd Int. Conf. on Electricity Distribution, Lyon, 2015

[8] Goergens, P., Potratz, F., Cramer, M., *et al.*: 'Review of the smart operator in the field'. CIRED Workshop, Helsinki, 2016

[9] Diop, F., Hennebel, M.: 'Probabilistic load flow methods to estimate impacts of distributed generators on a LV unbalanced distribution grid'. 2017 IEEE Manchester PowerTech, Manchester, United Kingdom, 2017, pp. 1–6